From Stellar to Laboratory Jets

Andrea Ciardi

andrea.ciardi@obspm.fr

LERMA
Observatoire de Paris, Université Pierre et Marie Curie, Ecole Normale Supérieure, CNRS UMR 8112

- - -


X-ray: NASA/CXC/CfA/R.Kraft et al.; Submillimeter: MPIfR/ESO/APEX/A.Weiss et al.; Optical: ESO/WFI

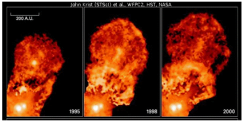
John Krist (STScI) et al., WFPC2, HST, NASA
200 A.U.
1995
1998
2000

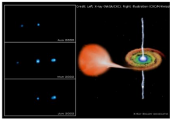

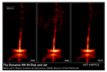

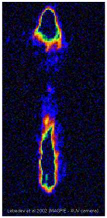
Lebedev et al 2002 (MAGPIE - XUV camera)

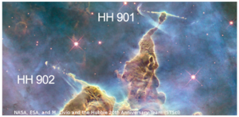
HH 901
HH 902
NASA, ESA, and M. Livio and the Hubble 20th Anniversary Team (STScI)


NASA/JPL-Caltech


Hen 3-1475 (ESA/NASA)

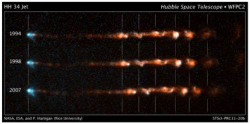
HH 34 Jet
Hubble Space Telescope • WFPC2
1994
1998
2007
NASA, ESA, and P. Hartigan (Rice University)
STScI-PRC11-20b

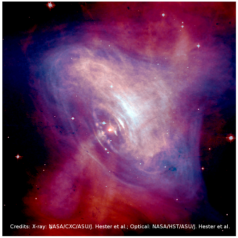
Credits: X-ray: NASA/CXC/ASU/J. Hester et al.; Optical: NASA/HST/ASU/J. Hester et al.


Ant Nebula, Menzel 3, Mz 3, NASA, ESA and The Hubble Heritage Team (STScI/AURA)
R. Sahai (Jet Propulsion Lab) and B. Balick (University of Washington)


M2-9
M2-9, Hubble 5, NGC 6537, (NASA).
Bruce Balick, Vincent Icke, Garrelt Mellema

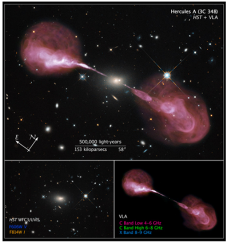
Hercules A (3C 348)
HST + VLA
500,000 light-years
153 kiloparsecs
58"
HST WFC3/UVIS
VLA

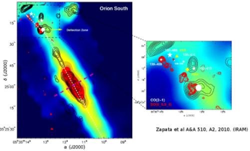
Orion South
Deflection Zone
α (J2000)
δ (J2000)
Zapata et al A&A 510, A2, 2010. (IRAM)

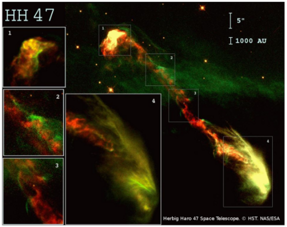
HH 47
5"
1000 AU
1
2
3
4
Herbig Haro 47 Space Telescope. © HST. NAS/ESA

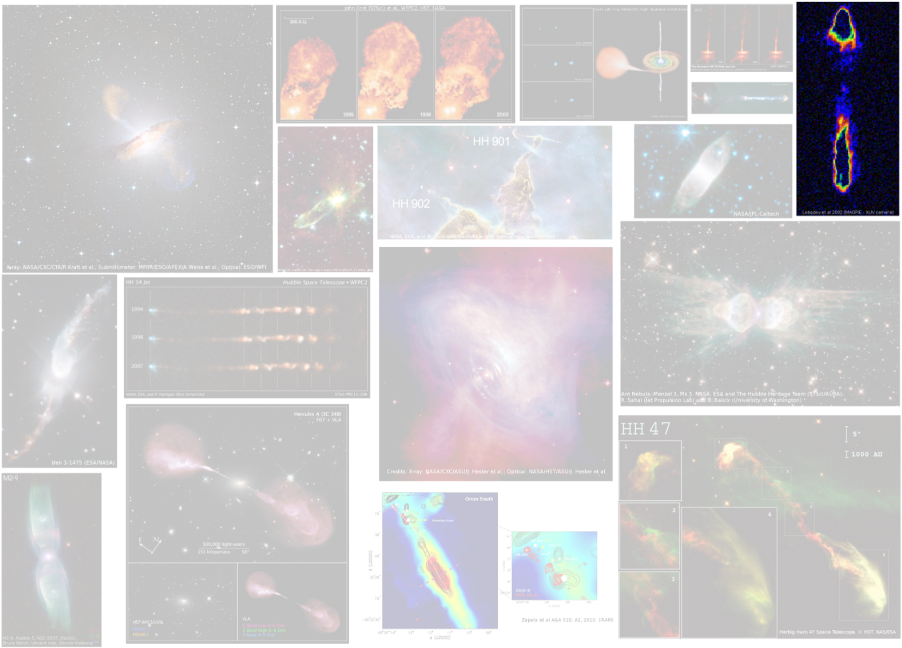

X-ray: NASA/CXC/CfA/R.Kraft et al.; Submillimeter: MPIfR/ESO/APEX/A.Weiss et al.; Optical: ESO/WFI
John Krist (STScI) et al., WFPC2, HST, NASA
200 A.U.
1995
1998
2000
HH 901
HH 902
NASA, ESA, and M. Livio and the Hubble 20th Anniversary Team (STScI)
NASA/JPL-Caltech
Lebedev et al 2002 (MAGPIE - XUV camera)
HH 34 Jet
Hubble Space Telescope • WFPC2
1994
1998
2007
NASA, ESA, and P. Hartigan (Rice University)
STScI-PRC11-20b
Hen 3-1475 (ESA/NASA)
Ant Nebula, Menzel 3, Mz 3, NASA, ESA and The Hubble Heritage Team (STScI/AURA)
R. Sahai (Jet Propulsion Lab) and B. Balick (University of Washington)
Credits: X-ray: NASA/CXC/ASU/J. Hester et al.; Optical: NASA/HST/ASU/J. Hester et al.
HH 47
5"
1000 AU
Herbig Haro 47 Space Telescope. © HST. NAS/ESA
M2-9
M2-9, Hubble 5, NGC 6537, (NASA)
Bruce Balick, Vincent Icke, Garrelt Mellema
Hercules A (3C 348)
HST + VLA
500,000 light-years
153 kiloparsecs
58"
HST WFC3/UVIS
VLA
Orion South
Zapata et al A&A 510, A2, 2010. (IRAM)

What jet physics can we study in the laboratory?

- Hydrodynamic and magneto-hydrodynamic instabilities (including radiation)
- Turbulent jets propagation and mixing with the ambient medium
- Generation of bow shocks and collision dynamics
- Aspects of magnetic jet formation and collimation

Warning from the past...

Symposium on Gas Dynamics of Cosmic Clouds, Cambridge 1953

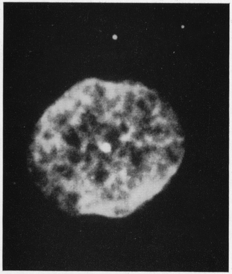

A

NGC 1501, a planetary nebula of apparently turbulent character. Estimated distance 3400 parsec; estimated diameter 0.9 parsec.

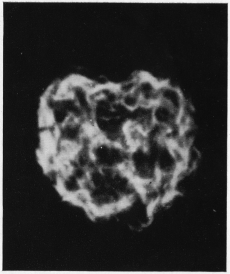

B

Flame propagation in a turbulent stream. Tenfold exposure of flame at 400 microseconds after ignition in a stream of turbulent gas with velocity 50 meters/second. Diameter 7 millimeters.

The similarity of these pictures may not mean a physical similarity of the processes involved.

Warning from the past...

Symposium on Gas Dynamics of Cosmic Clouds, Cambridge 1953

. . . to bring together workers from astrophysics and from aerodynamics. . .

. . . to consider which developments in fluid mechanics may be applicable to astrophysical problems. . .

Warning from the past...

Symposium on Gas Dynamics of Cosmic Clouds, Cambridge 1953

...to bring together workers from astrophysics and from aerodynamics...

...to consider which developments in fluid mechanics may be applicable to astrophysical problems...

- Attendees to the conference included
  - B. J. Bok, E. Schatzman, G.K. Batchelor, H. Bondi, F. Hoyle, D.W. Sciama, G.I. Taylor, L. Mestel, M.J. Seaton, T.G. Cowling, J.M. Burgers, Th. von Karman, J.H. Oort...E. Fermi & S. Chandrasekhar

Warning from the past...

Symposium on Gas Dynamics of Cosmic Clouds, Cambridge 1953

. . . to bring together workers from astrophysics and from aerodynamics. . .

. . . to consider which developments in fluid mechanics may be applicable to astrophysical problems. . .

- Attendees to the conference included
  - B. J. Bok, E. Schatzman, G.K. Batchelor, H. Bondi, F. Hoyle, D.W. Sciama, G.I. Taylor, L. Mestel, M.J. Seaton, T.G. Cowling, J.M. Burgers, Th. von Karman, J.H. Oort...E. Fermi & S. Chandrasekhar

1. First symposium "Problems of Cosmical Aerodynamics" was held in Paris in 1949
2. "Gas Dynamic of Cosmic Clouds" Cambridge, UK 1953
3. "Cosmical Gas Dynamics", Cambridge, USA, 1957
4. "Cosmical Gas Dynamics: Aerodynamic Phenomena in Stellar Atmospheres", Varenna, Italy, 1960
5. The Fifth Symposium on Cosmical Gas Dynamics, Nice, France, 1965
6. .....

The first “astrophysics experiments” on flow dynamics

- A. Kantrowitz (Cornell University) “Experiments on the Radiation and Ionization Produced by Strong Shocks Waves”
  - “In the identification of shocks waves and in determining the role of shock phenomena in astrophysics, laboratory studies of strong shocks waves can make a contribution”

The first "astrophysics experiments" on flow dynamics

- A. Kantrowitz (Cornell University) "Experiments on the Radiation and Ionization Produced by Strong Shocks Waves"
  - "In the identification of shocks waves and in determining the role of shock phenomena in astrophysics, laboratory studies of strong shocks waves can make a contribution"

- W. Bostick (Lawrence Livermore) "Possible Hydromagnetic Simulation of Cosmical Phenomena in the Laboratory"

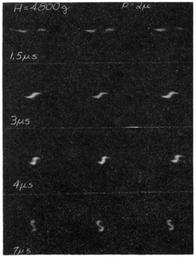

  - *Discussed the scaling to astrophysical phenomena*

Alfvén scaling...

from his book "Cosmic Electrodynamics", 1950

Problem	*Linear dimension*	*Density particles/cm.^{3}*	*Magnetic field gauss*	*Time*
Aurora and magnetic storms . . . Reduced: $\eta = 3.10^8$.	3.10^9 10	10^3 ?–10^{12} 3.10^{11} ?–3.10^{20}	0·5–0·01 1·5.10^8–3.10^6	Initial phase of storm = 3h. = 10^4 sec. → 30 μsec.
Solar corona . . . Reduced: $\eta = 10^{10}$–10^{11}	10^{11}–10^{12} 10	10^8–10^6 10^{18}–10^{17}	20–0·02 2.10^{11}–2.10^9	Life of coronal arc = 10^3 sec. → 10^{-7} sec. Solar cycle = 11 years = 3.10^8 sec. → 0·03 sec.
Chromosphere . . Reduced: $\eta = 10^8$.	10^9 10	10^{11}–10^{14} 10^{19}–10^{22}	20 2.10^9	Solar flare 1,000 sec. → 10 μsec. Prominence 10^5 sec. → 1,000 μsec.
Planetary system . . Reduced: $\eta = 10^{12}$–10^{13}	10^{13}–10^{14} 10	10^3 ? 10^{15}–10^{16} ?	10^{-5}–10^{-8} 10^7–10^5	1 year → 3–30 μsec.
Galaxy . . . . Reduced: $\eta = 3.10^{21}$.	3.10^{22} 10	1 3.10^{21}	10^{-12} ? 3.10^9 ?	Age of universe = 10^{10} years = 3.10^{17} sec. → 100 μsec.

Plan of the talk

- Jets in young stars
  - Divide jet physics into hydrodynamics and magneto-hydrodynamics
- High-energy density installation (laser and z-pinch)
- Modelling of astrophysical jets and designing MHD jet experiments
  - Simplifications needed to study magnetic jet formation and collimation experimentally
- Hydrodynamic jets: propagation and interaction with an ambient medium

Jets/outflows during low-mass star formation

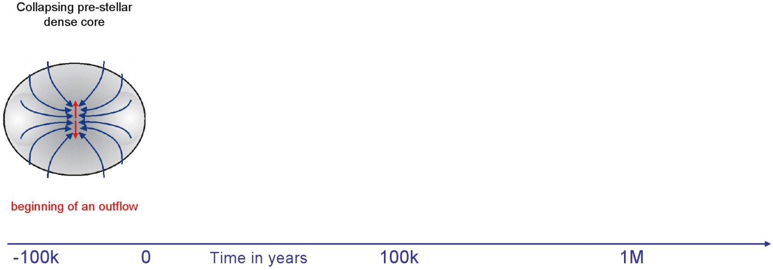

Core size few $\times 10^4$ AU
Mass core $\sim$ few $\times M_\odot \gg M_\star$
$\dot{M}_{acc} \sim 10^{-4}$ $M_\odot$ year^{-1}

Jet/Outflow:

- First evidence (?) of an outflow from an adiabatic core
- Estimated age 200 years
- Slow, few km/s outflow

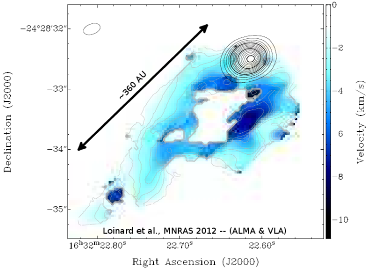

Jets/outflows during low-mass star formation

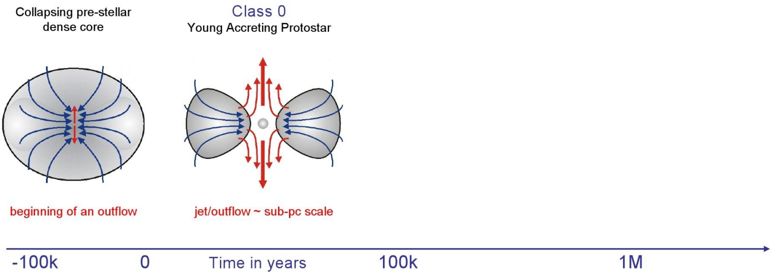

Envelope $\sim$ 1000 AU
Mass envelope/disk $> M_\star$
$\dot{M}_{acc} \sim 10^{-5}$ $M_\odot$ year^{-1}

Jet/Outflow:

- ▷ Atomic jet close to the source
- ▷ Mostly observed as (swept up) molecular flows
  - ▸ Slow ($v \lesssim 10$ km/s) cavities
  - ▸ Fast ($v \sim 10 - 100$ km/s) jet/bullets

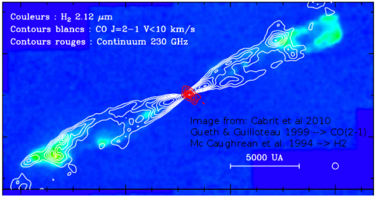

Jets/outflows during low-mass star formation

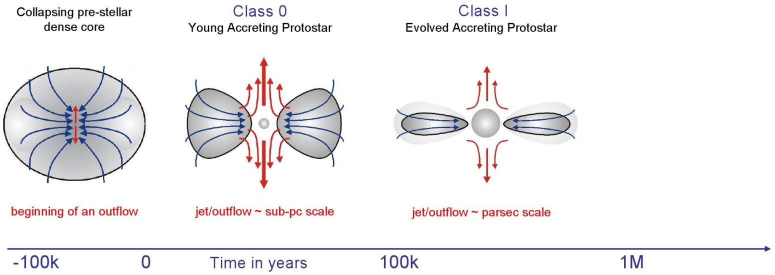

Disk/envelope size *few* $\times$ 100 AU
Mass envelope/disk $< M_\star$
$\dot{M}_{acc} \sim 10^{-6}$ $M_\odot$ year^{-1}

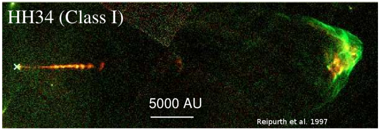

Jet/Outflow:

- Atomic jet traced to pc-scales
- Weaker swept up molecular flow
- Clear evidence jet episodicity and variability

Jets/outflows during low-mass star formation

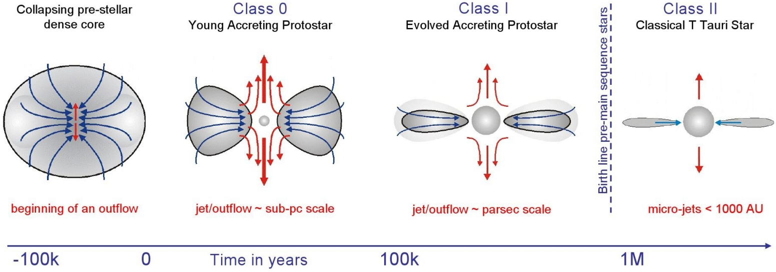

Disk size $\lesssim 100$ AU
Mass disk $\ll M_\star$
$\dot{M}_{acc} \lesssim 10^{-7}\ \mathrm{M}_\odot\ \mathrm{year}^{-1}$

Jet/Outflow:

- Fast, several 100 km/s atomic jets
- Wide-angle, slow H_2
- Rapid (few years) jet variability

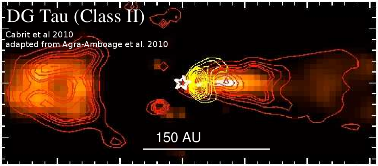

Simplifying is the key

hydrodynamic vs. magneto-hydrodynamic jets

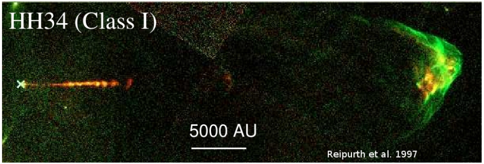

TABLE 1

Average Jet Parameters

Distance from Star (AU)	Arcseconds[a]	n^{b} (cm^{-3})	$B_{\perp}$	V_A[c] (km s^{-1})
10	0.02	2.5×10^6	82 mG	113
30	0.06	1.5×10^6	53 mG	94
100	0.2	4.5×10^5	19 mG	62
300	0.6	8.8×10^4	4.8 mG	35
10^3	2.2	10^4	0.75 mG	16
3×10^3	6.5	1.2×10^3[d]	124 μG[d]	7.8
10^4	22	110[d]	16 μG[d]	3.3
3×10^4	65	12[d]	2.4 μG[d]	1.5

[a] Spatial offset from the star at the distance of the Orion star-forming region (460 pc).

[b] Densities for a conical flow with a half opening angle of 5° and a base width of 10 AU, taking the density to be 10^4 cm^{-3} at 1000 AU.

[c] The Alfvén speed V_A determined from the total density n.

[d] Values refer to an average density; densities at large distances are highly influenced by shocks and rarefaction waves. See text.

Hartigan et al 2007

Simplifying is the key

hydrodynamic vs. magneto-hydrodynamic jets

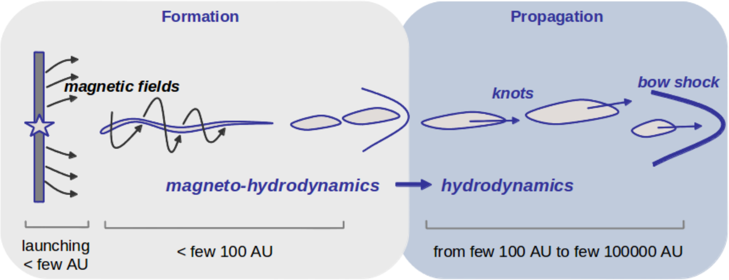

- **Formation –> Magneto-hydrodynamics**
  - Essentially only on z-pinches and one new expt. on laser
- **Propagation –> Hydrodynamics**
  - Many experiments on lasers and z-pinches

High-energy density plasma (HEDP) facilities

Working definition: energy density $\varepsilon \gtrsim 10^{12}\,\mathrm{erg\,cm^{-3}}$; pressure $p \gtrsim 1\,\mathrm{Mbar}$

Lasers

- Energy: $\sim 1 - 10^4\,\mathrm{J} \rightarrow$ MJ
- time-scales 10s of ns
- plasma volumes $\sim$ mm^3

Pulsed-power generators (z-pinch)

- Energy: 100 J to several MJ
- Time-scales 100s ns
- Plasma volumes $\sim$ cm^3

laser facilities

Vulcan UK

LIL France

FIREX Japan

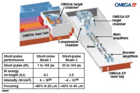

OMEGA USA

Mega Joule Facilities

NIF USA

LMJ France

pulsed-power facilities

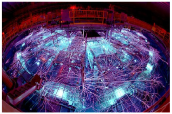

Z-machine in the USA has 11.4 MJ of stored energy and delivers a 20 MA current in 100 ns

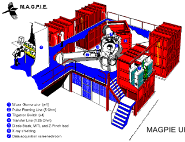

MAGPIE UK

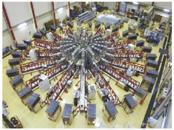

SPHYNX France

ZEBRA USA

For a review of HEDP laboratory astrophysics experiments see Remington et al 2006

High-energy density plasmas

Working definition: energy density $\varepsilon \gtrsim 10^{12}\,\mathrm{erg\,cm^{-3}}$; pressure $p \gtrsim 1\,\mathrm{Mbar}$

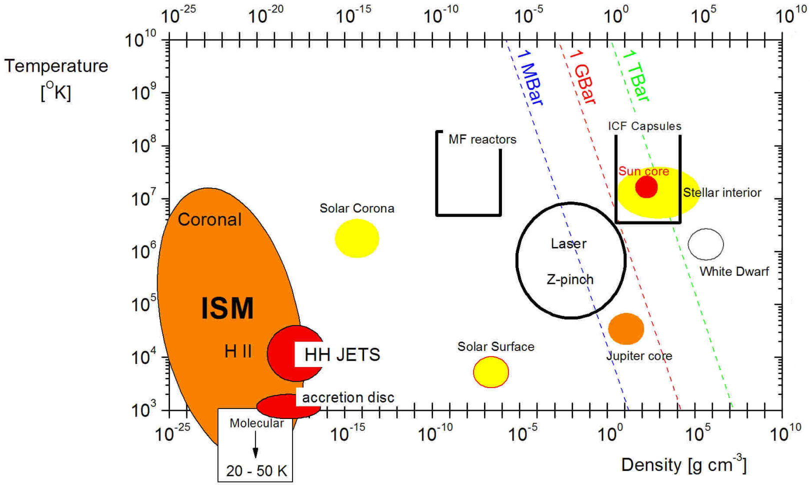

High-energy density plasmas

Working definition: energy density $\varepsilon \gtrsim 10^{12}\,\mathrm{erg\,cm^{-3}}$; pressure $p \gtrsim 1\,\mathrm{Mbar}$

"Nominal" plasma conditions (laser):

- Length scale $L \sim 0.1$ cm
- Temperatures $T \sim 500$ eV
- Density $\rho \sim 10^{-3}\,\mathrm{g\,cm^{-3}}$
- Bulk flow speed $v \sim 500$ km/s
- $\lambda_{mfp} \ll L$
- $B \sim 0.1$ MG
- $\beta \sim 10^6$
  - in general $\beta \ll 1$ to $\beta \gg 1$

Magneto-hydrodynamic jets

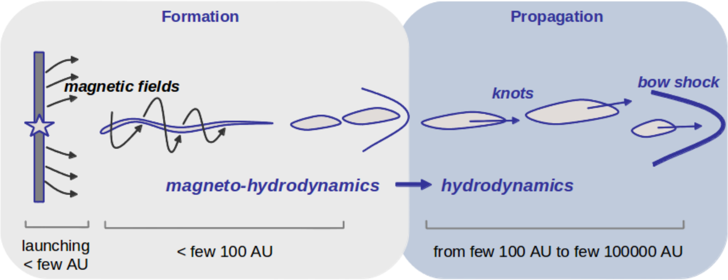

Basics of jet launching[1]

From the (axisymmetric) induction equation:

$$\frac{\partial B_\phi}{\partial t} = -r\mathbf{B_{pol}} \cdot \nabla\omega(\mathbf{r}, \mathbf{z})$$

differential angular rotation, ω, along an initially poloidal field line, $\mathbf{B_{pol}}$, generates an azimuthal component B_ϕ.

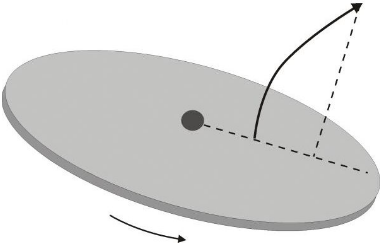

[1]Blandford & Payne 1982; Pelletier et al 1992; Ferreira 1995 & 1997; ....

Basics of jet launching[1]

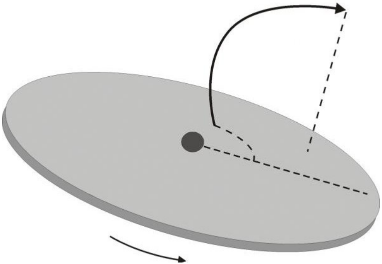

[1] Blandford & Payne 1982; Pelletier et al 1992; Ferreira 1995 & 1997; ....

Basics of jet launching[1]

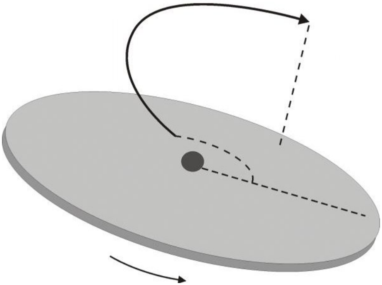

[1]Blandford & Payne 1982; Pelletier et al 1992; Ferreira 1995 & 1997; ....

Basics of jet launching[1]

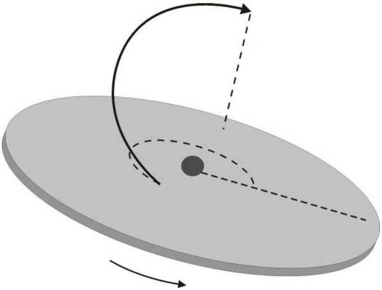

[1] Blandford & Payne 1982; Pelletier et al 1992; Ferreira 1995 & 1997; ....

Basics of jet launching[1]

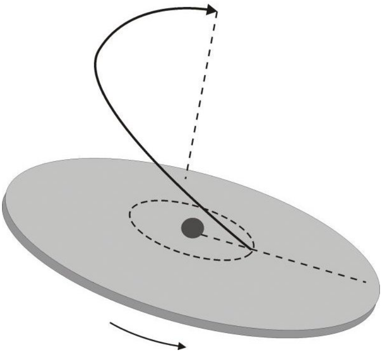

[1] Blandford & Payne 1982; Pelletier et al 1992; Ferreira 1995 & 1997; ....

Basics of jet launching[1]

Magnetic force on the plasma $\mathbf{F} = \mathbf{j} \times \mathbf{B}$:

Azimuthal:

$$F_\phi = \frac{B_{pol}}{\mu_0 r} \nabla_\parallel (rB_\phi)$$

Poloidal:

$$F_\parallel = -\frac{B_\phi}{\mu_0 r} \nabla_\parallel (rB_\phi)$$

$$F_\perp = -\frac{B_\phi}{\mu_0 r} \nabla_\perp (rB_\phi) + B_{pol} J_\phi$$

Current (field) distribution is fundamental:

$$I = \frac{2\pi}{\mu_0} rB_\phi$$

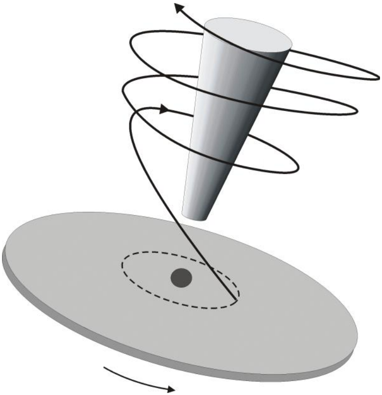

[1] Blandford & Payne 1982; Pelletier et al 1992; Ferreira 1995 & 1997; ....

Basics of jet numerical modelling

Collapsing prestellar dense-cores[2]

- ▷ Early stages (few thousand years) of jet evolution
- ▷ Essentially limited to slow outflow components (protostar either not there or just formed)
- ▷ 2D and 3D "self-consistent" jet/disk system

$$\frac{\partial \rho}{\partial t} = -\nabla \cdot (\rho \mathbf{v})$$

$$\rho \frac{\partial v}{\partial t} + (\rho \mathbf{v}) \cdot \nabla \mathbf{v} = -\nabla p + \frac{\mathbf{j} \times \mathbf{B}}{c} - \rho \nabla \Phi + \text{ non-ideal terms}$$

$$\frac{\partial \epsilon}{\partial t} + \nabla \cdot (\epsilon \mathbf{v}) = -\, p \nabla \cdot \mathbf{v} + \text{non-ideal terms}$$

$$\frac{\partial \mathbf{B}}{\partial t} = \nabla \times (\mathbf{v} \times \mathbf{B}) + \text{non-ideal terms}$$

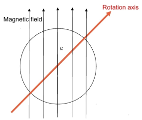

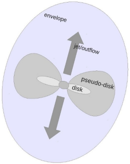

sR

[2] Machida et al 2006; Banerjee & Pudritz 2006; Mellon & Li 2008; Hennebelle & Fromang 2008; Hennebelle & Ciardi 2009; Ciardi & Hennebelle 2010; Joos et al 2012

Basics of jet numerical modelling

Disk included (and star)[2]

- ▷ Start with an initial star-disk/ambient structure and large-scale poloidal field
- ▷ Essentially limited to 2D and relatively short time-scales
- ▷ Jets can have a feedback on the disk and star

$$\frac{\partial \rho}{\partial t} = -\nabla \cdot (\rho \mathbf{v})$$

$$\rho \frac{\partial v}{\partial t} + (\rho \mathbf{v}) \cdot \nabla \mathbf{v} = -\nabla p + \frac{\mathbf{j} \times \mathbf{B}}{c} - \rho \nabla \Phi - \nu \nabla^2 \mathbf{v}$$

$$\frac{\partial \epsilon}{\partial t} + \nabla \cdot (\epsilon \mathbf{v}) = -\, p \nabla \cdot \mathbf{v} - \Lambda_{rad} + \Lambda_{Ohm} + \Lambda_{visc}$$

$$\frac{\partial \mathbf{B}}{\partial t} = \nabla \times (\mathbf{v} \times \mathbf{B} - \eta_m \nabla \times \mathbf{B})$$

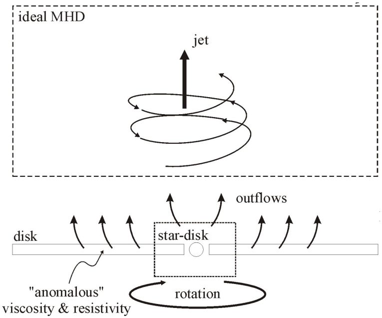

[2] Kudoh et al 1998; Zanni et al. 2007; Bessolaz et al 2008; Zanni & Ferreira 2012

Basics of jet numerical modelling

Disk (or Poynting flux injection) as a boundary condition[2]

- Field distribution, rotation and mass injection at the base of the jet are imposed
- No jet/wind feedback on the disk
- 2D and 3D over long time and spatial scales
- May neglect gravity

$$\frac{\partial \rho}{\partial t} = -\nabla \cdot (\rho \mathbf{v})$$

$$\rho \frac{\partial v}{\partial t} + (\rho \mathbf{v}) \cdot \nabla \mathbf{v} = -\nabla p + \frac{\mathbf{j} \times \mathbf{B}}{c}$$

$$\frac{\partial \epsilon}{\partial t} + \nabla \cdot (\epsilon \mathbf{v}) = -\, p \nabla \cdot \mathbf{v} - \Lambda_{rad}$$

$$\frac{\partial \mathbf{B}}{\partial t} = \nabla \times (\mathbf{v} \times \mathbf{B})$$

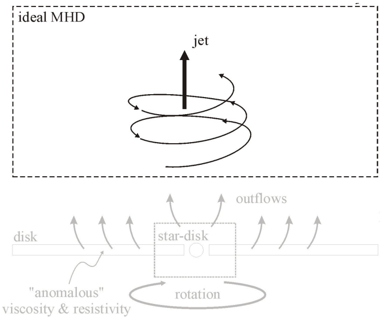

[2] Ouyed & Pudritz 1997; Ustyugova 1999; Anderson et al 2005; Fendt 2006; Matsakos et al 2009

Modelling jets in the laboratory

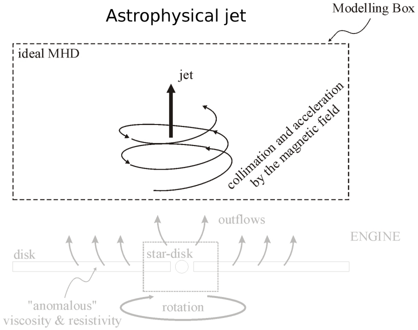

To design a laboratory astrophysics jet experiments requires:

1. ideal MHD to be applicable
2.

Modelling jets in the laboratory

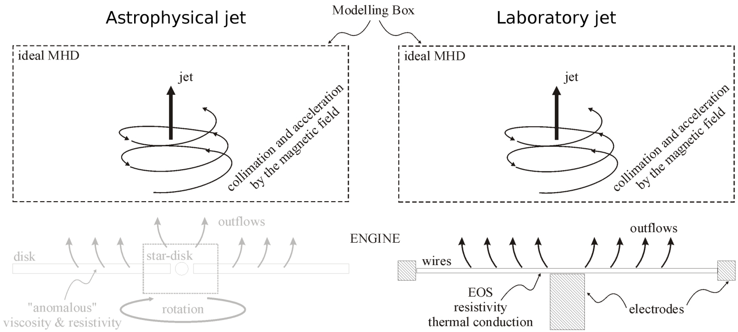

To design a laboratory astrophysics jet experiments requires:

1. ideal MHD to be applicable
2. Relevant initial/boundary conditions

Modelling jets in the laboratory

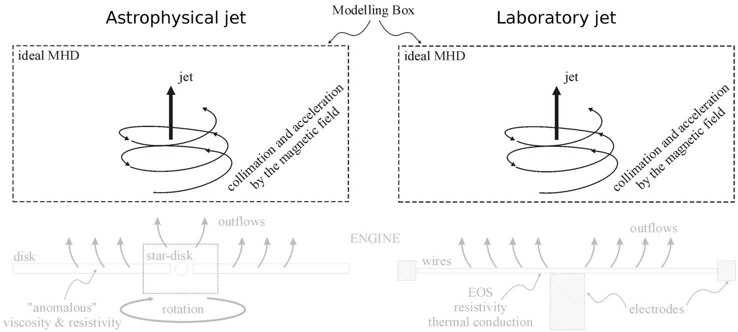

To design a laboratory astrophysics jet experiments requires:

1. ideal MHD to be applicable
2. Relevant initial/boundary conditions

Modelling jets as ideal-magnetofluids

$$\frac{\partial \rho}{\partial t} = -\nabla \cdot (\rho \mathbf{v})$$

$$\rho \frac{\partial v}{\partial t} + (\rho \mathbf{v}) \cdot \nabla \mathbf{v} = -\nabla p + \frac{\mathbf{j} \times \mathbf{B}}{c} - \nu \nabla^2 \mathbf{v}$$

$$\frac{\partial \epsilon}{\partial t} + \nabla \cdot (\epsilon \mathbf{v}) = -p\nabla \cdot \mathbf{v} - \nabla \cdot \mathbf{q} - \Lambda_{rad} + \Lambda_{Ohm} + \Lambda_{visc}$$

$$\frac{\partial \mathbf{B}}{\partial t} = \nabla \times (\mathbf{v} \times \mathbf{B} - \eta_m \nabla \times \mathbf{B})$$

From non-ideal to ideal MHD

- Reynolds number

$$\mathrm{Re} = \frac{vL}{D_{visc}} \gg 1$$

- Magnetic Reynolds number

$$\mathrm{Re}_m = \frac{vL}{D_m} \gg 1$$

- Peclet number

$$\mathrm{Pe} = \frac{vL}{D_T} \gg 1$$

Scaling laboratory astrophysics experiments [3]

Transformations of the ideal (M)HD equation

Ideal MHD equation (without gravity)

$$\frac{\partial \rho}{\partial t} = -\nabla \cdot (\rho \mathbf{v})$$

$$\rho \frac{\partial v}{\partial t} + (\rho \mathbf{v}) \cdot \nabla \mathbf{v} = -\nabla p + \mathbf{j} \times \mathbf{B}$$

$$\frac{\partial p}{\partial t} + \nabla \cdot (p \mathbf{v}) = -(\gamma - 1) p \nabla \cdot \mathbf{v} - (\gamma - 1) \Lambda_{rad}$$

$$\frac{\partial \mathbf{B}}{\partial t} = \nabla \times (\mathbf{v} \times \mathbf{B})$$

$$p = C \rho^{\varsigma} T^{\nu}$$

$$\Lambda_{rad} = \Lambda_0 p^{\chi} \rho^{\xi}$$

[3] Ryutov et al 2000, 2001; Falize et al 2010, 2009; Bouquet et al 2011

Scaling laboratory astrophysics experiments [3]

Transformations of the ideal (M)HD equation

Ideal MHD equation (without gravity)

$$\frac{\partial \rho}{\partial t} = -\nabla \cdot (\rho \mathbf{v})$$

$$\rho \frac{\partial v}{\partial t} + (\rho \mathbf{v}) \cdot \nabla \mathbf{v} = -\nabla p + \mathbf{j} \times \mathbf{B}$$

$$\frac{\partial p}{\partial t} + \nabla \cdot (p\mathbf{v}) = -(\gamma - 1) p \nabla \cdot \mathbf{v} - (\gamma - 1)\Lambda_{rad}$$

$$\frac{\partial \mathbf{B}}{\partial t} = \nabla \times (\mathbf{v} \times \mathbf{B})$$

$$p = C \rho^{\varsigma} T^{\nu}$$

$$\Lambda_{rad} = \Lambda_0 p^{\chi} \rho^{\xi}$$

Transformation:

$$X = \lambda^{\delta_i} \tilde{X}$$

where λ^{δ_i} are the scaling parameters.
For example:

$$r = \lambda^{\delta_1} \tilde{r}$$
$$t = \lambda^{\delta_2} \tilde{t}$$
$$\mathbf{v} = \lambda^{\delta_3} \mathbf{v}$$
$$\ldots$$

One obtains a set of constraints on the scaling parameters.

- In general the number of constraints is smaller than the number of scaling parameters, allowing a certain flexibility.

[3] Ryutov et al 2000, 2001; Falize et al 2010, 2009; Bouquet et al 2011

High-energy density plasmas

Working definition: energy density $\varepsilon \gtrsim 10^{12}\,\mathrm{erg\,cm^{-3}}$; pressure $p \gtrsim 1\,\mathrm{Mbar}$

Nominal plasma conditions (laser):

- Length scale $L \sim 0.1$ cm
- Temperatures $T \sim 500$ eV
- Density $\rho \sim 10^{-3}\,\mathrm{g\,cm^{-3}}$
- $B \sim 0.1$ MG
- Bulk flow speed $v \sim 500$ km/s
- $\lambda_{mfp} \ll L$
- $\beta \sim 10^6$
  - in general $\beta \ll 1$ to $\beta \gg 1$)
- Mach number $M \gtrsim 3$
- Pe ~ 15
- Re $\sim 10^6$
- $\mathrm{Re}_M \sim 600$

Laboratory vs. Simulations vs. The real thing

Approximating the ideal-MHD equations

	Stellar jets	Simulations	Laboratory
Re	10^{12}	$10 - 10^3$	$> 10^5$
Re_m	10^{16}	$10 - 10^3$	$10 - 10^3$
Pe	10^{10}	$10 - 10^3$	$10 - 10^3$

$$\chi = \frac{\tau_{cool}}{\tau_{hydro}} = \frac{1}{\tau_{hydro}} \times \frac{\varepsilon}{\Lambda_{rad}} < 1$$

Compressible, radiative magneto-hydrodynamic flows in the laboratory

Laboratory vs. Simulations vs. The real thing

Approximating the ideal-MHD equations

	Stellar jets	Simulations	Laboratory
Re	10^{12}	$10 - 10^3$	$> 10^5$
Re_m	10^{16}	$10 - 10^3$	$10 - 10^3$
Pe	10^{10}	$10 - 10^3$	$10 - 10^3$

$$\chi = \frac{\tau_{cool}}{\tau_{hydro}} = \frac{1}{\tau_{hydro}} \times \frac{\varepsilon}{\Lambda_{rad}} < 1$$

Compressible, radiative magneto-hydrodynamic flows in the laboratory

What about the initial/boundary conditions?

“Poloidal” versus “Toroidal” collimation

Collimating and accelerating force components

$$F_{\parallel} = -\frac{B_{\phi}}{\mu_0 r} \nabla_{\parallel} (rB_{\phi})$$

$$F_{\perp} = -\frac{B_{\phi}}{\mu_0 r} \nabla_{\perp} (rB_{\phi}) + B_{pol} J_{\phi}$$

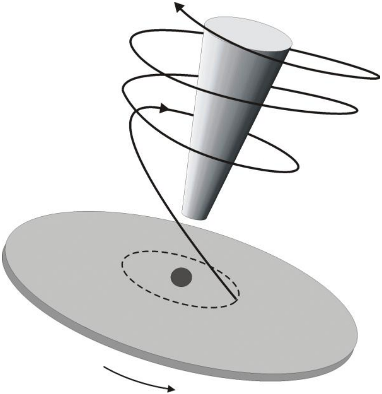

Experiments to investigate

1. $B_{\phi} \gg B_{pol} \rightarrow$ *acceleration* and *collimation* by toroidal component

2. $B_{pol} \gg B_{\phi} \rightarrow$ *collimation* by poloidal component

The basic ingredients to make a jet

To model jet formation in the laboratory seems to require at least (differential) rotation and an initially poloidal magnetic field

1. At a certain distance from the source where $v_p \sim v_{p_A} = \left(B_p/\sqrt{4\pi\rho}\right)$:

$$B_\phi \gg B_p$$

2. Current distributions are important. The circuit needs to be closed within the outflow $\longrightarrow$ need for an *ambient medium*

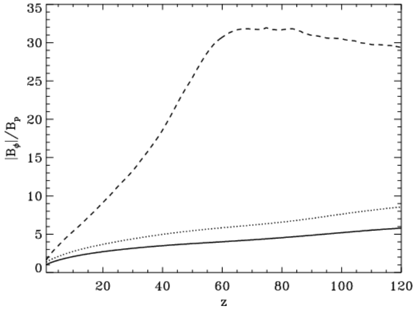

(Images credit: Zanni et al A&A 2007)

The basic ingredients to make a jet

To model jet formation in the laboratory seems to require at least (differential) rotation and an initially poloidal magnetic field

1. At a certain distance from the source where $v_p \sim v_{pA} = \left(B_p/\sqrt{4\pi\rho}\right)$:

$$B_\phi \gg B_p$$

2. Current distributions are important. The circuit needs to be closed within the outflow $\longrightarrow$ need for an *ambient medium*

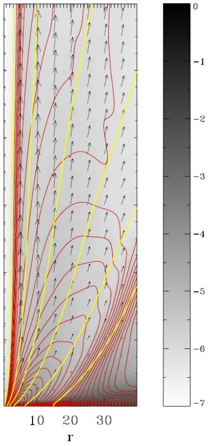

(Images credit: Zanni et al A&A 2007)

The basic ingredients: B_ϕ and a plasma

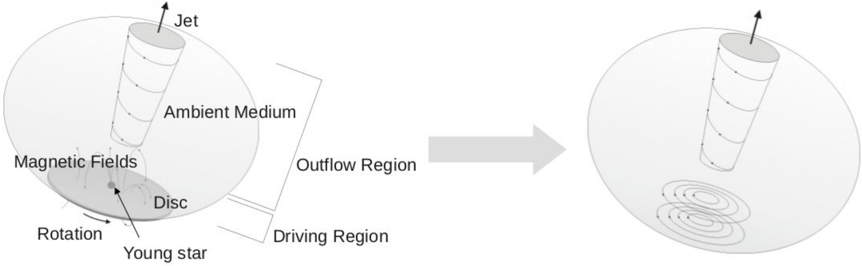

An example of astrophysical simulations with $B_\phi \gg B_{pol}$

Early phases of star formation[4]

Magnetized wind into an ambient density distribution from analytical, isothermal collapse models.

$$B_\phi \sim r^{-1} \qquad \rho \sim r^{-2} \qquad v = \text{const}$$

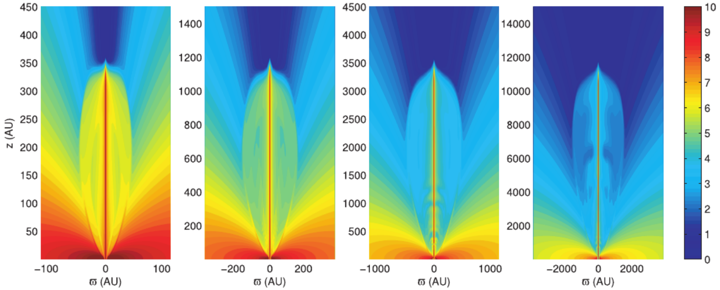

[4] Shang et al ApJ 2006

Formation of magnetized laboratory jets[5]

- ▷ Pulsed-current generator
  - MAGPIE generator Imperial College
  - currents several $1 - 1.4$ MA
- ▷ Load
  - thin metallic wires or foil (few - few $\times$ 10 μm)
  - material: aluminium, copper, tungsten....
- ▷ Time-scale few hundred nanoseconds
- ▷ Length-scale few cm of plasma

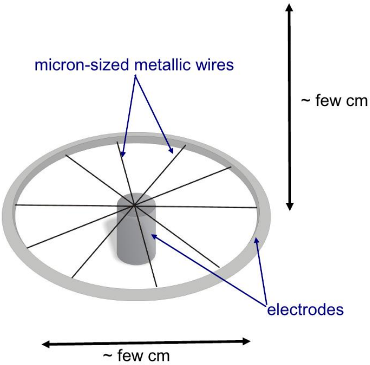

[5] Lebedev et al 2005, Ciardi et al 2005

Formation of magnetized laboratory jets[5]

Below wires/foil the magnetic field is purely azimuthal:

$$B_\phi \sim \frac{1}{r}$$

Force on **ablated** plasma is (mostly) axial:

$$F_z = -\frac{\partial}{\partial z}\left(\frac{B_\phi^2}{8\pi}\right)$$

wire cores / cold foil remain stationary

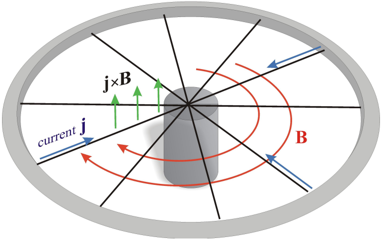

[5] Lebedev et al 2005, Ciardi et al 2005

Formation of magnetized laboratory jets[5]

Ambient medium

- $v \sim 100$ km/s
- $n \sim 10^{18}$ cm^{-3}
- $T \sim 10$ eV ($\sim 10^5$ K)
- Mostly free of current and magnetic field

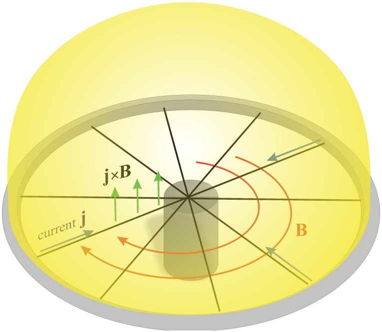

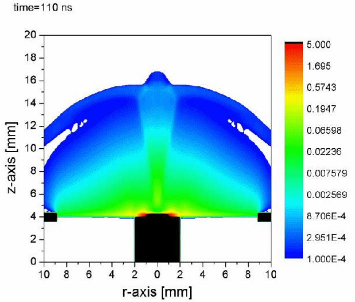

[5] Lebedev et al 2005, Ciardi et al 2005

Formation of magnetized laboratory jets[5]

Ablation is faster near the central electrode:

$$\frac{dm}{dt} \propto \frac{1}{r}$$

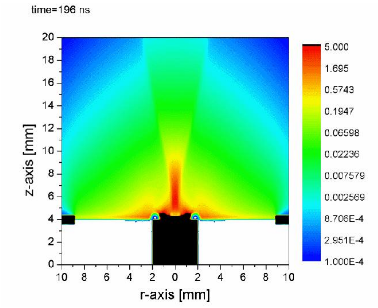

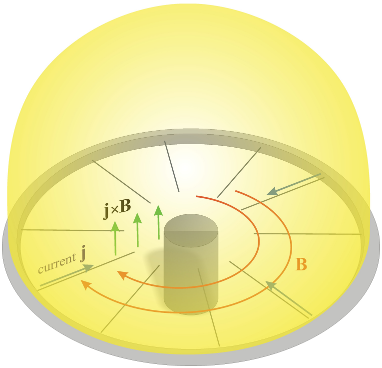

[5] Lebedev et al 2005, Ciardi et al 2005

Formation of magnetized laboratory jets[5]

Rising magnetic bubble:

- Magnetic bubble is confined/collimated by the ambient plasma
- A *magnetized* jet forms on the axis, collimated by the magnetic field

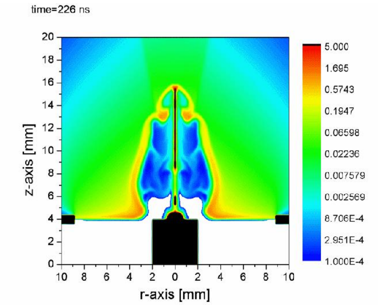

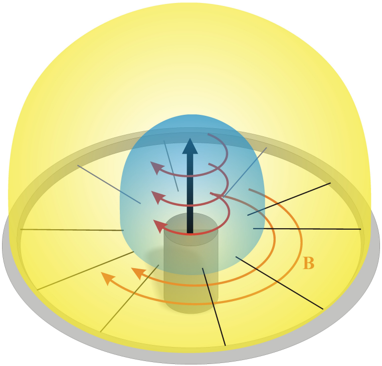

[5] Lebedev et al 2005, Ciardi et al 2005

From stellar to laboratory jets

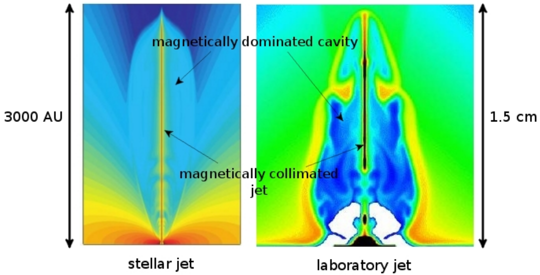

- ▷ Magnetically collimated jet
- ▷ Magnetically dominated cavity ($\beta \ll 1$) confined by the *external medium*
- ▷

From stellar to laboratory jets

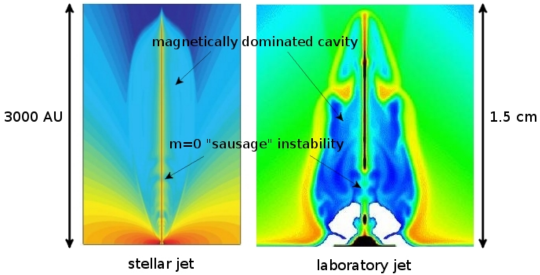

- Magnetically collimated jet
- Magnetically dominated cavity ($\beta \ll 1$) confined by the *external medium*
- $m = 0$ “sausage” instability

From stellar to laboratory jets...not quite yet

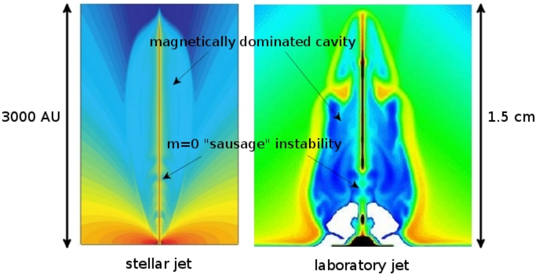

- ▷ Magnetically collimated jet
- ▷ Magnetically dominated cavity ($\beta \ll 1$) confined by the *external medium*
- ▷ $m = 0$ "sausage" instability

However reality is not axisymmetric....

Experiments and 3D simulations show kink-unstable jets[6]

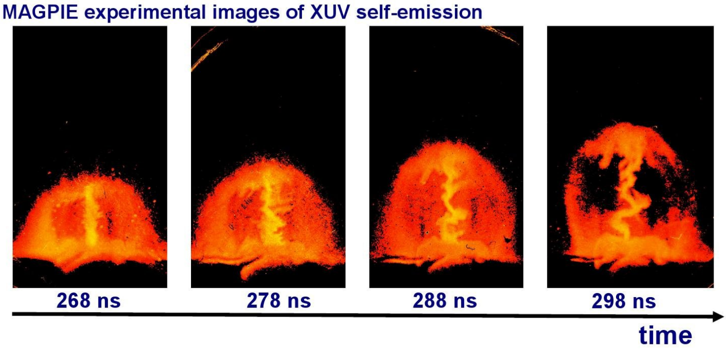

[6] Lebedev et al 2005; Ciardi et al 2007

Experiments and 3D simulations show kink-unstable jets[6]

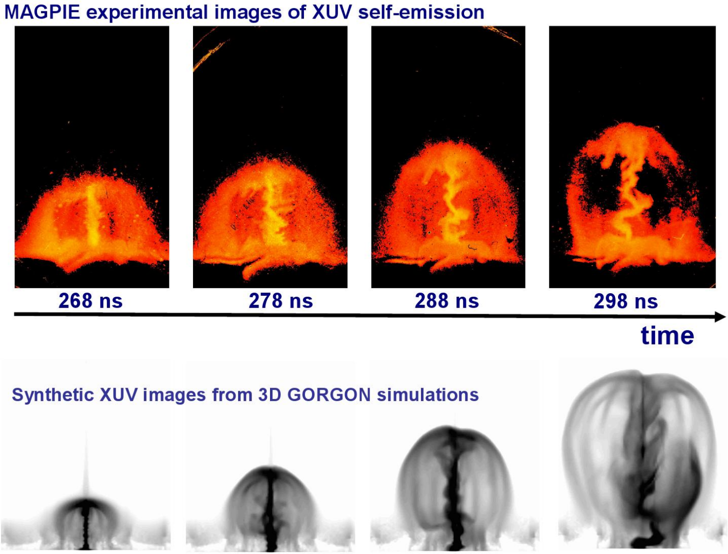

[6] Lebedev et al 2005; Ciardi et al 2007

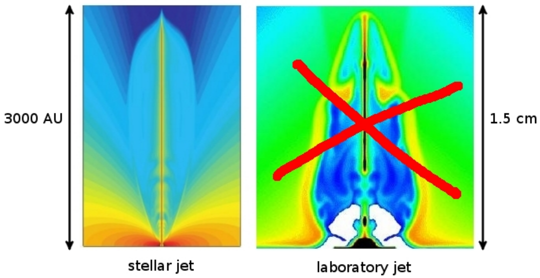
3000 AU
1.5 cm
stellar jet
laboratory jet

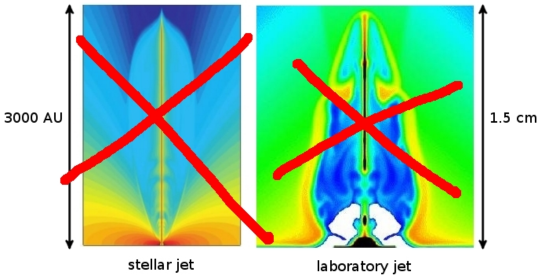
3000 AU
1.5 cm
stellar jet
laboratory jet

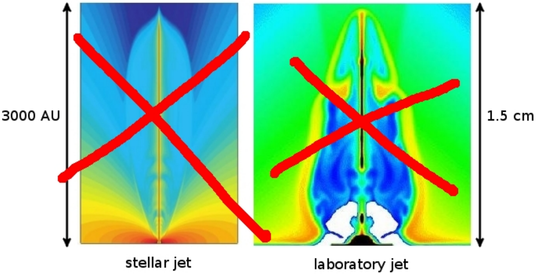

$B_z \neq 0 \quad \rightarrow$ stability

Kink instability in astrophysical jets[7]

Linear analysis of **idealized-jet configuration:**

- For jets with $\beta \ll 1$
  - the $m = 1$ mode is the fastest growing
  - unsheared field leads to body modes
  - sheared field leads to internal modes
- For jets with $\beta \gg 1$
  - fastest growing modes can be for $m \gg 1$ corresponding to very large k_z
  - short-wavelengths $\rightarrow$high-resolution $\rightarrow$ difficult to simulate
- In general the growth rate

$$\gamma \sim v_{A\phi}/R_j$$

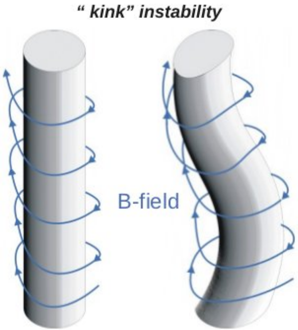

[7] Appl et al A&A 2000; Bonanno et al A&A 2010 ...

Mounting evidence that jets become unstable

Nakamura et al 2003

- Poynting Flux Dominated jets
- Kink $m = 1$ mode dominates
- *No instability for low resolution simulations*
- Rotation can help stabilize the jet (within the computational domain)
  - Unmagentized *rotating* jets have been produced on z-pinches (Ampleford et al 2008)

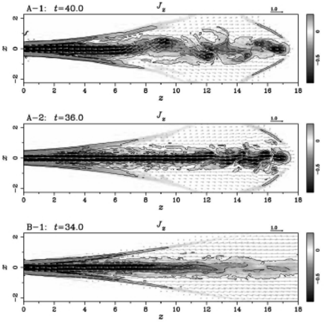

Moll et al 2008

- Followed the jet over very long length-scales ($2000 \times R_{j0}$)
- Kink instability always develops
- Differential rotation helps to reduce growth rate

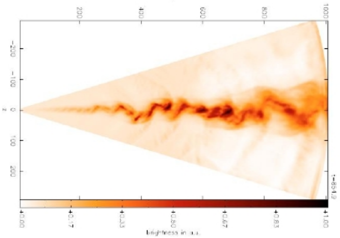

Poynting-dominated magnetic tower jets[8]

3D AMR MHD simulations with AstroBEAR

1. Kink instability appears first in the cooling jet.
   - Cooling increases growth rate as in laboratory jets
2. Rotation has a destabilizing effect.
   - At odd with previous findings, however the set-up is different
   - Possible to test in the laboratory

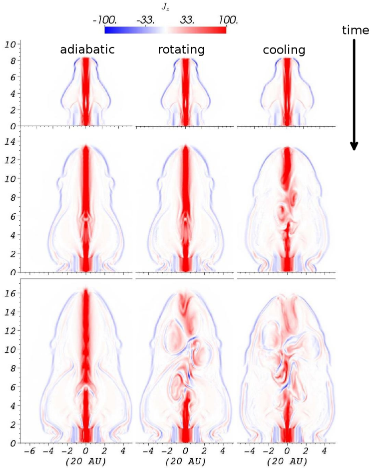

[8] Huarte-Espinosa et al ApJ 2012

Pre-protostellar jets[9]

3D AMR MHD simulations with RAMSES

Follow the gravitational collapse of a dense (10^6 cm^{-3}) pre-stellar core of 1 $M_\odot$.

Range of magnetizations and misalignments α.

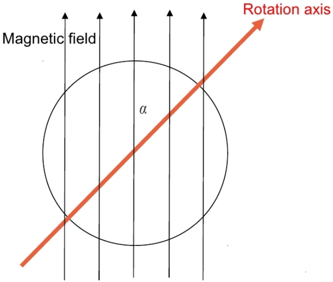

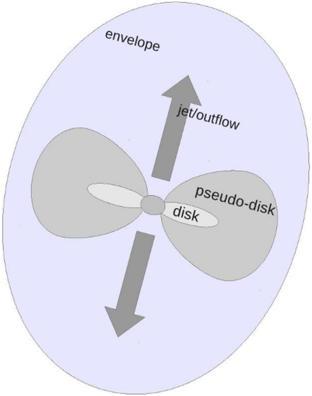

[9]Hennebelle & Ciardi 2009; Ciardi & Hennebelle 2010; Joos et al 2012, 2013

Pre-protostellar jets[10]

3D AMR MHD simulations with RAMSES

- Bulk velocities $v \sim 1 - 5$ km/s
- For increasing α
  - lower mass ejections rates
  - no jets/outflows for $\alpha \sim 90^\circ$
  - more heterogeneous flows

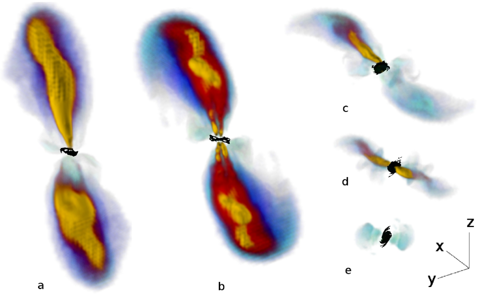

[10] Hennebelle & Ciardi 2009; Ciardi & Hennebelle 2010; Joos et al 2012, 2013

On-going work: kink-instability in pre-protostellar jets

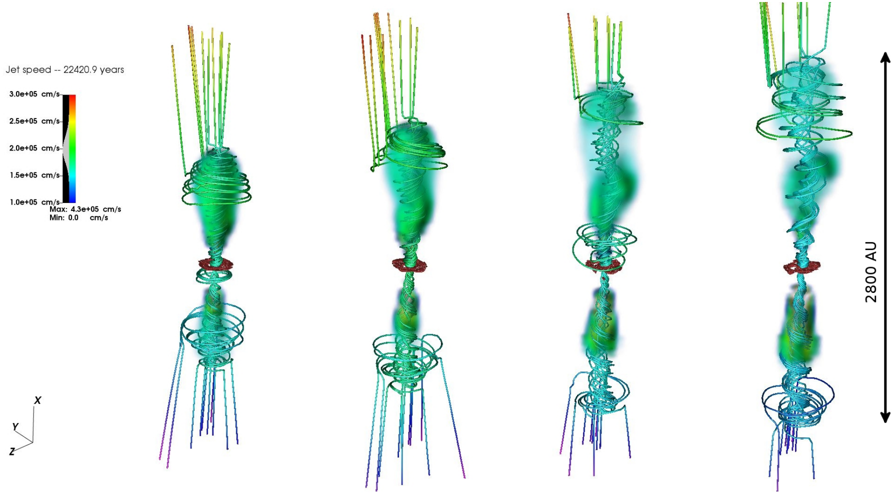

Aligned case $\alpha = 0^\circ$

Are these instabilities destructive?

Kink instability in laboratory jets

Helical perturbation modifies the direction of the current generating a poloidal component of the field

$$B_\phi \gg B_P \quad \rightarrow \quad B_\phi \sim B_p$$

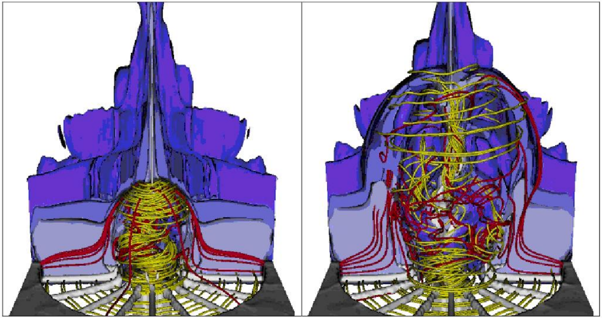

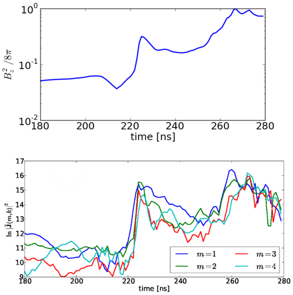

Clumpy jets from toroidally dominated flows

Kink-instability is non-destructive

- Kinetically dominated clumps
  - High Mach number $M_{fms} > 5$
  - High collimation $\alpha \sim 5^\circ$
  - $B_\phi \sim B_z \sim B_r$

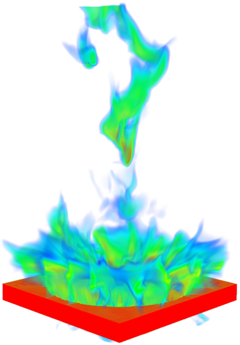

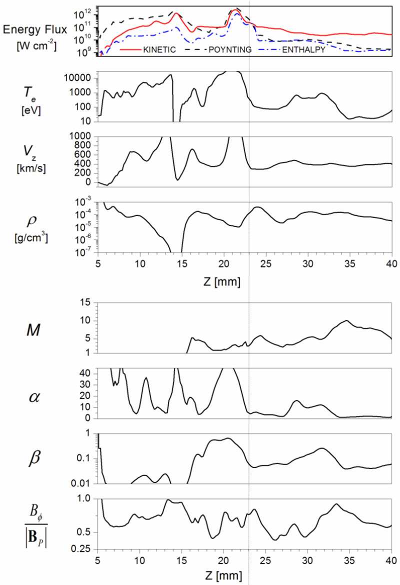

On-going work: scaling to other experimental devices

Experiments performed with radial wire arrays on a the **CEA-GRAMAT** long-current pulse ($\sim 1.4\,\mu$s) **Oedipe** machine (800 kA).

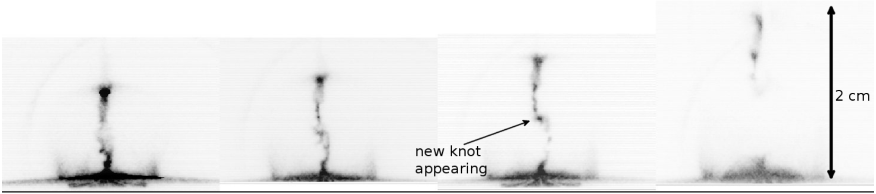

Smaller amplitude perturbations of the jet body.

- ▷ Indications that Poynting flux into cavity was suddenly halted (wire gap filled by plasma?).
- ▷ Cavity/jet expansion may be freezing out the instabilities.

Schematic formation of episodic laboratory jets

Replace wires by a metallic micron-sized foil

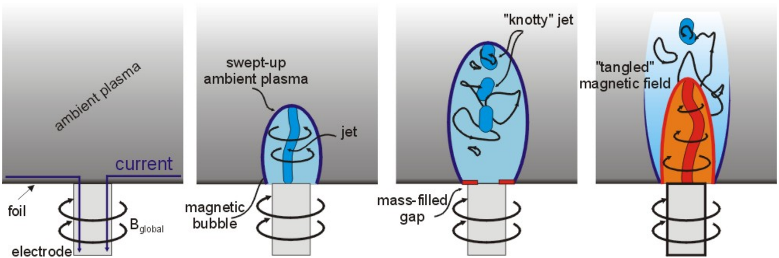

Episodic jets: the experiments[11]

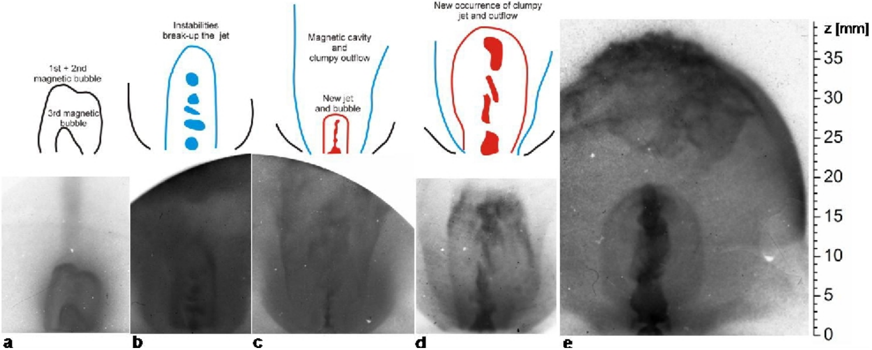

- ▷ Episodic ejections create a "self-collimating" channel with a clumpy jet on the interior
  - Each magnetic cavity is confined by previously ejected plasma and field
  - No memory of initial conditions

[11] Ciardi et al 2009; Suzuki-Vidal et al 2009 & 2010

Phenomenological model

Back to space from the laboratory

$$X_{astro} = A_i X_{lab}$$

Scaling factors

$A_v = 1$
$A_\rho = 8 \times 10^{-15}$
$A_t = 3 \times 10^{-15}$
$A_x = A_v A_t = 3 \times 10^{-15}$
$A_p = A_\rho A_v^2 = 8 \times 10^{-15}$
$A_B = \sqrt{A_p} = 9 \times 10^{-8}$

Physical variables

	Astro	Lab
v	10^7 cm/s	10^7 cm/s
n	10^6 cm^{-3}	10^{19} cm^{-3}
t	1 year	10 ns
x	21 AU	1 mm
p	10^{-10}	16 kbar
B	1 mG	1 T
χ_{cool}	< 1	< 1

Phenomenological model

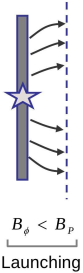

Distance from source $D \lesssim$ few$\times$AU
Steady-state jet launching

Phenomenological model

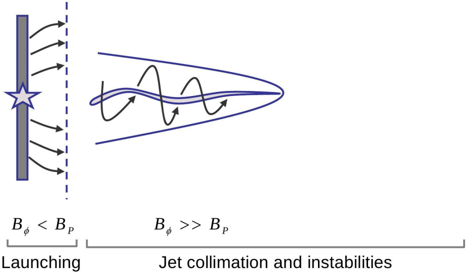

Distance from source $D \lesssim$ few$\times$100 AU
Flow is structured by instabilities

Phenomenological model

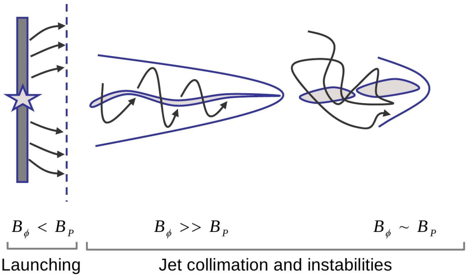

Distance from source $D \lesssim$ few$\times$100 AU
Flow is structured by instabilities
Substantial flow inhomogeneities: ρ, T and $\mathbf{v}$.
Decay and tangling of the field.

Phenomenological model

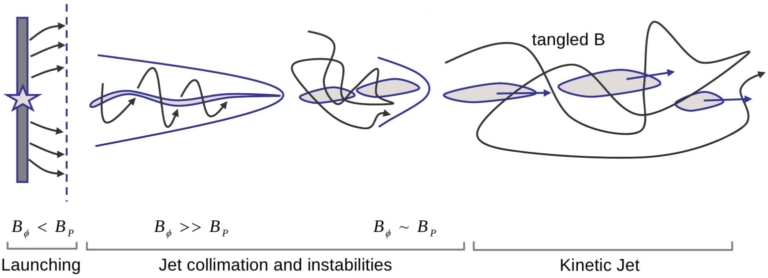

Distance from source $D \gtrsim$ few$\times$100 AU
Flow is kinetically dominated
Interaction between clumps producing internal shocks
Interaction with previously ejected material or the ISM

Phenomenological model

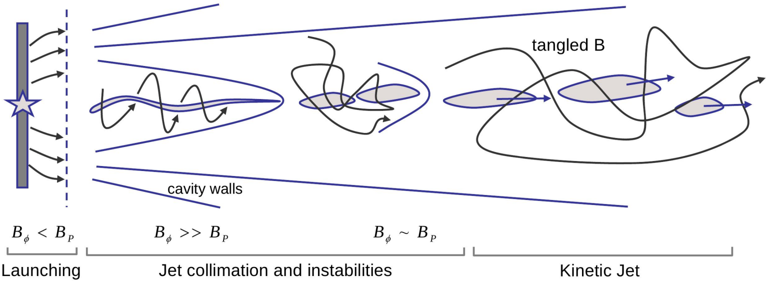

Presence of bubble/cavity like features

Poloidal collimation

Collimating and accelerating force components

$$F_{\parallel} = -\frac{B_\phi}{\mu_0 r}\nabla_{\parallel}(rB_\phi)$$

$$F_{\perp} = -\frac{B_\phi}{\mu_0 r}\nabla_{\perp}(rB_\phi) + B_{pol}J_\phi$$

Experiments to investigate

1. $B_\phi \gg B_{pol} \rightarrow$ *acceleration* and *collimation* by toroidal component
2. $B_{pol} \gg B_\phi \rightarrow$ *collimation* by poloidal component

Astrophysical and laboratory context

Poloidal collimation[12]

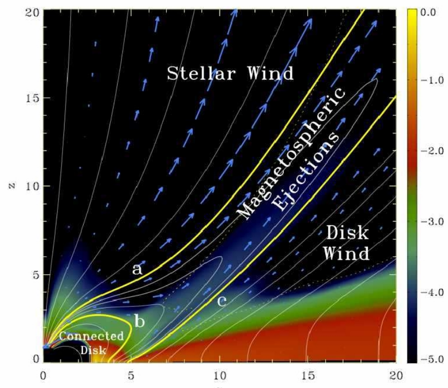

Zanni & Ferreira, A&A 2012

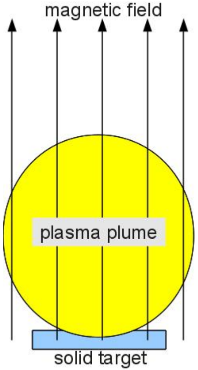

[12] Spruit et al 1997; Matt et al 2003; Romanova et al 2009

Laser-driven plasma plume → thermally-driven wind

Simulation shown has no magnetic field

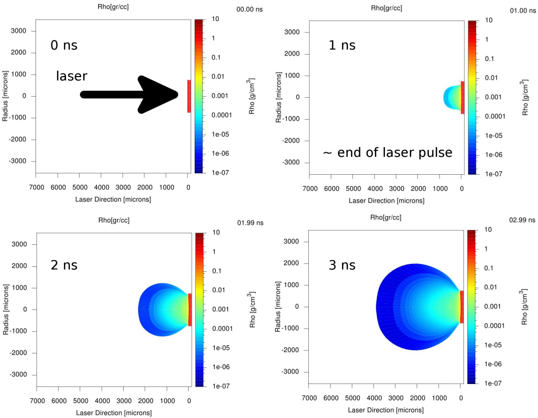

- Laser-target interaction with the 2D Lagrangian, radiation hydrodynamics code DUED *(Atzeni et al 2005)*
    - Profiles then input in our 3D resistive MHD code GORGON

Magnetically collimated laser-generated plasmas[13]

Poloidal collimation

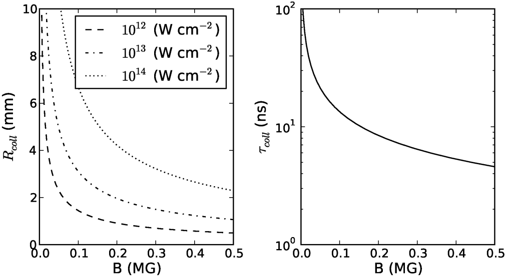

Nominal laser parameters:

$E_L = 50 - 500$ J ; $\tau_L = 1$ ns; $\lambda = 1.064\,\mu\mathrm{m}$; $\phi = 750\,\mu\mathrm{m}$

Estimates of the magnetic filed strength and its duration:
$B_0 \gtrsim 0.1$ MG for several $t \gg 10$ ns

[13] Ciardi et al 2013

Magnetically collimated laser-generated plasmas

1. Cavity-shell formation
   - High-beta cavity
   - Formation of a shell of shocked material and compressed **B**
   - Re-direction of plasma along cavity walls

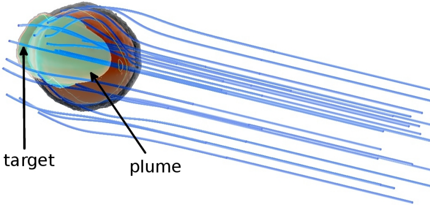

2. Jet formation
   - Re-directed flow converges towards the axis
   - Formation of a conical shock
   - Axial re-direction and jet formation

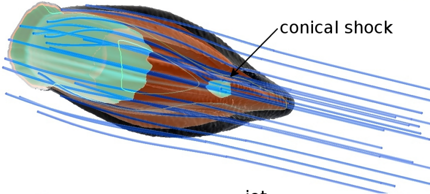

3. Re-collimation
   - Secondary cavity
   - Re-collimation, conical shock and jet

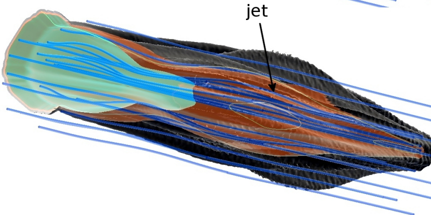

Magnetically collimated laser-generated plasmas

$I \sim 10^{14}\,\mathrm{W\,cm^{-2}}$ and $B_0 \sim 0.2\,\mathrm{MG}$

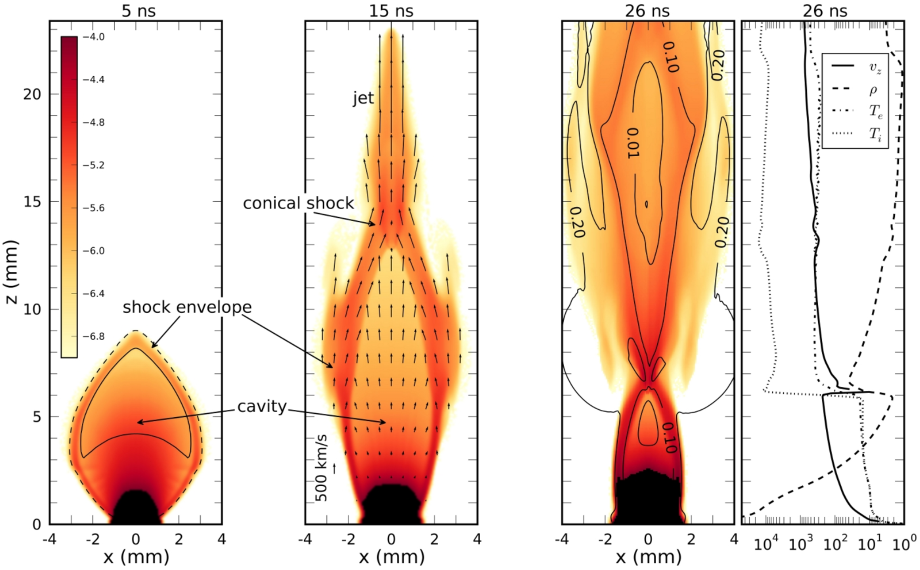

Flow instabilities

Rayleigh-Taylor type filamentation instability[14]

Configuration similar to a θ-pinch

- Growth rate

$$\gamma \sim \sqrt{g k_\theta}$$

$$k_\theta = m/R_{jet}$$

$$g \sim v^2/R_C$$

- Growth time-scale is short

$$\tau_I \sim \frac{\tau_{coll}}{\sqrt{m}} \sim \text{few ns}$$

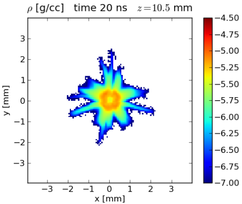

[14] *Kleev & Velikovich 1990*

Flow instabilities

Firehose[15]

Jet may be susceptible to firehose instability

$$P_{\parallel} - P_{\perp} > \frac{B^2}{4\pi}$$

$$P_{\parallel} \sim \rho v^2$$

$$M_A^2 - \frac{\beta}{3} > 1$$

Marginally stable for some combination of laser intensity and magnetic field

- Possible Kelvin-Helmoltz
- Electrons may are highly-magnetized → possible anisotropic thermal pressure
- Possible stabilization by the surrounding dense, magnetized plasma

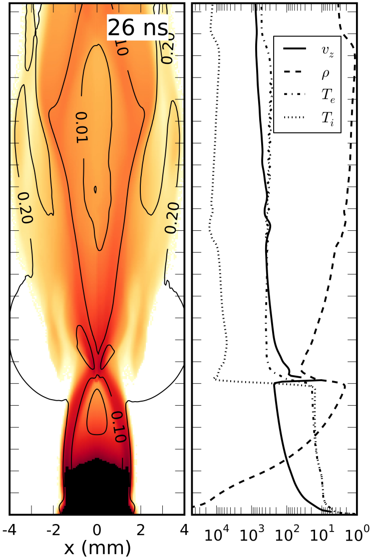

[15] *e.g. Benford 1981*

Hydrodynamic jets

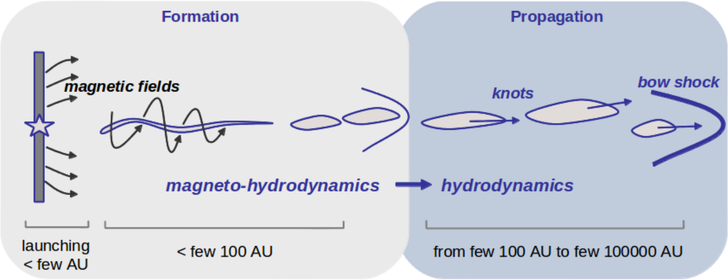

Converging flows to produce hydrodynamic jets

- ▷ Supersonically converging flows can generate conical/oblique shocks which focus the flow into a jet.
- ▷ This is the most common mechanism to generate hydrodynamic jets experimentally

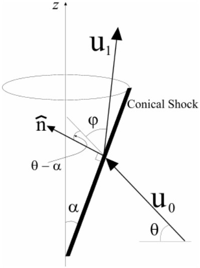

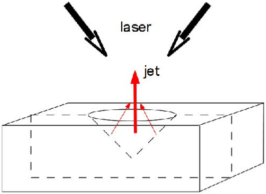

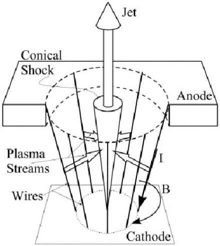

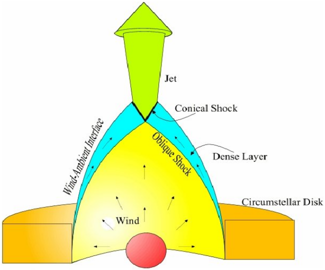

Early experiments on the Nova and GEKKO-XII lasers

Multi-beams - Total laser energy $\sim$ 500 J and 1 kJ in a 100 ps pulse ($I \sim 10^{14} - 10^{15}$ W cm^{-2})

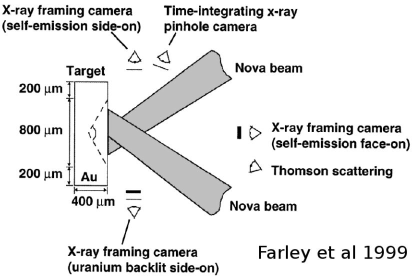

Farley et al 1999

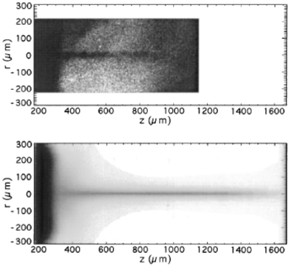

Farley et al 1999

Early experiments focused on characterising and developing basic understanding of jets

- ▷ Typical jet parameters:
  - Mach > 10
  - Re, Pe $>> 1$
- ▷ Radiative cooling plays an important role in the jet collimation

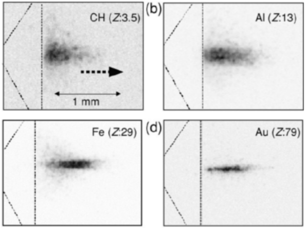

Shigemori et al 2000

Jets on the LULI2000 laser (Loupias 2007)

Multi-beams - Total laser energy $\sim$ 500 J to 1 kJ in a 1.5 ns pulse ($I \sim 10^{14}$ W cm^{-2})

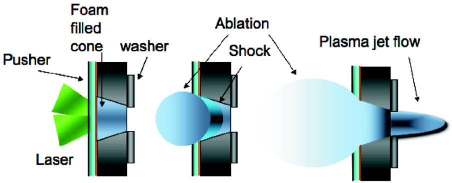

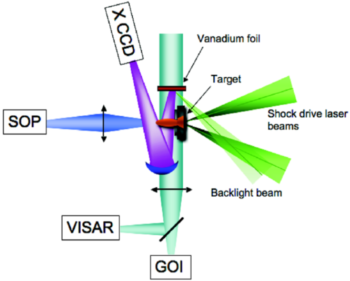

Rear-side illumination of target $\rightarrow$ easier to place an ambient medium

Simultaneous measurements of many jet parameters:

- ▷ SOP $\rightarrow$ temperature $\sim$ a few eV
- ▷ VISAR $\rightarrow$ velocities $\sim$ 100 km/s
- ▷ Radiography $\rightarrow$ densities $\lesssim$ 0.5 g cm^{-3}

Typical dimensionless parameters

- ▷ Mach $\sim$ 10
- ▷ Re, Pe >> 1

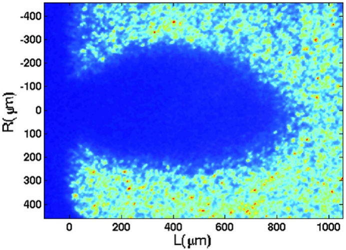

Jets on the PALS laser (Nicolai et al 2007, 2010; Kasperczuk et al 2006, 2011)

Single-beam - Total laser energy 13 – 160 J in a 250 ps pulse ($I \lesssim 10^{14}$ W cm^{-2})

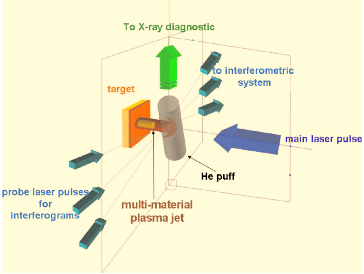

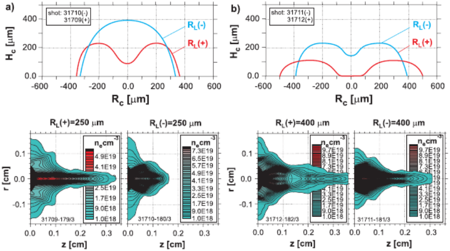

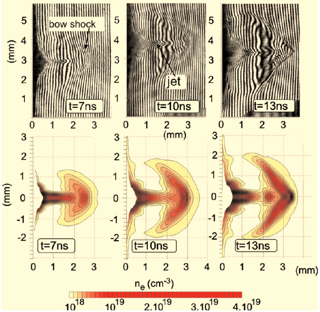

- ▷ Flat target with a laser focal spot that is double-peaked
- ▷ Low energy, single beam
- ▷ Began studying jet propagation (interaction)
- ▷ Not sure it works on other laser systems

Jets on the Omega laser (Foster et al 2005)

Multi-beams - Total laser energy $\sim$ 3.5 kJ in a 1 ns pulse ($I \sim 5 \times 10^{14}$ W cm^{-2})

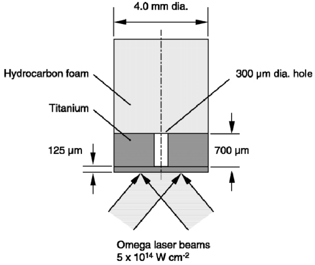

- ▷ Detailed studies with radiography
- ▷ Jet are relatively slow, dense and cold (close to liquid state):
  - $v \sim$10 km/s
  - $T \sim 3$ eV
  - $\rho \sim 0.1$ g cm^{-3}
  - Mach ~ 3 and Re and Pe >> 1

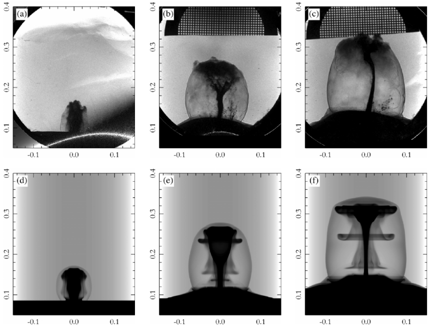

FIG. 2.—Experimental radiographs at (*a*) 100, (*b*) 200, and (*c*) 300 ns after the onset of the laser drive showing the primary (evident at 100 ns) and secondary (smaller diameter, evident at 200 ns and later) titanium jets. The dome-shaped pedestal results from shock transit through the titanium/foam interface. We also show transmission radiographs from simulations with RAGE in (*d*), (*e*), and (*f*). The diameters of the pedestal and jets, and the diameter of the bow shock in the low-density foam surrounding the jet, have been well captured, although a small offset and scaling of the times were necessary, which we attribute to small inaccuracies in the calculation of the pressure produced by the laser beams.

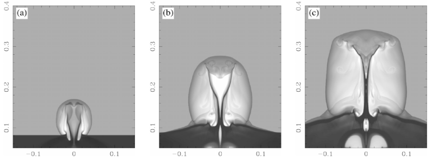

FIG. 3.—Fluid density from the RAGE calculations at (*a*) 100, (*b*) 200, and (*c*) 300 ns. The gray scale is logarithmic, from 10^{-2} to $10^{1.5}$ cm^{-3}; the axes are labeled in centimeters.

Deflected supersonic jets on the Omega laser (Hartigan et al 2009)

12 beams with a total energy of 6 kJ in 1 ns

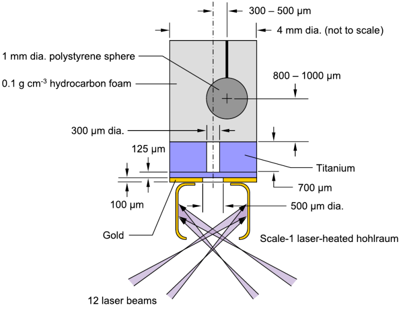

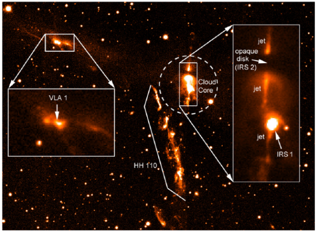

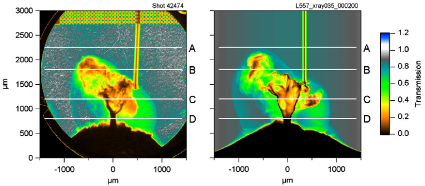

- ▷ Indirect drive: radiation temperature in the hohlraum 190-200 eV
- ▷ Study the fluid dynamics of the collision with a dense cloud.
- ▷ Detailed comparison with simulations
  - ▸ and observations

Jets on z-pinch machines (Lebedev et al 2002, 2004, 2005; Ciardi et al 2002)

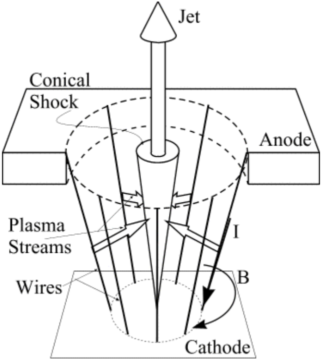

- Jets over long time- and length-scales $> 10\times$ laser experiments
- Similar dimensionless parameters to laser experiments
- More flexible:
  - rotating jets

Experiments on the CEA-GRAMAT z-pinch

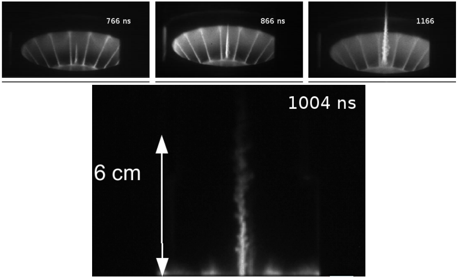

Rotating jets on twisted conical arrays (Ampleford et al 2008)

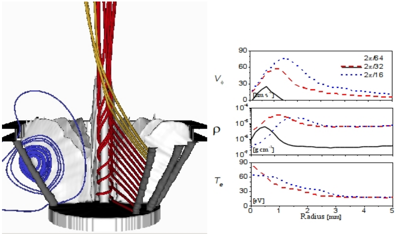

Curved jets on z-pinch machines

(Lebedev et al 2004, Ampleford et al 2007, Ciardi et al 2008)

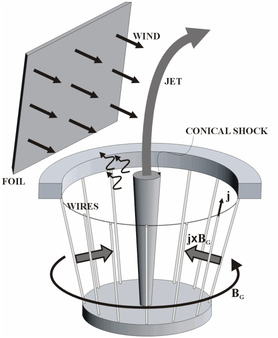

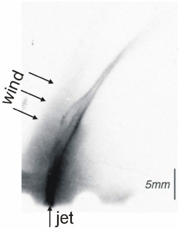

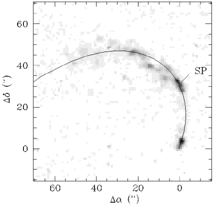

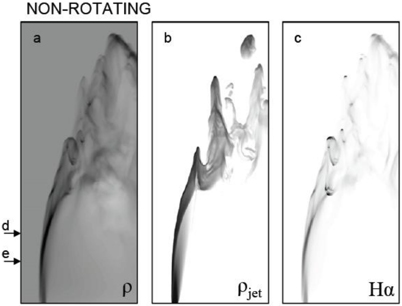

- ▷ Astrophysical context: motion of source wrt interstellar medium
- ▷ Jet is susceptible to RT instability
  - ▸ formation of clumps and internal shocks
  - ▸ rotation stabilizes the jet

Bow shocks studies on z-pinches (Suzuki-Vidal et al 2012)

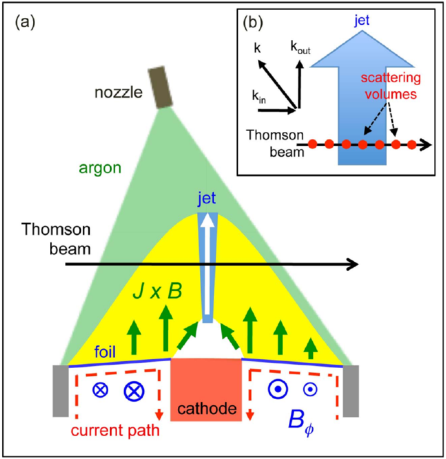

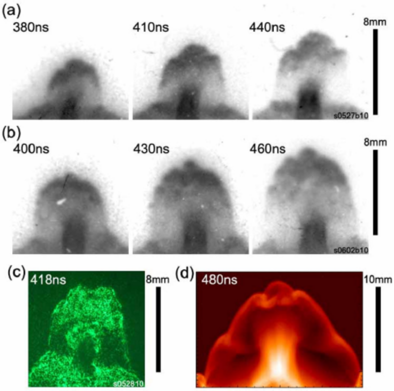

Jet velocities ~ 50-100 km/s

Conclusions

- Experiments can study a range of physics relevant to jets
  - Hydrodynamic and magneto-hydrodynamic instabilities (including radiation)
  - Turbulent jets propagation and mixing with the ambient medium
  - Generation of bow shocks and collision dynamics
  - Aspects of magnetic jet formation and collimation
- Many experiments in their infancy
  - so expect more interesting results
- Important to couple experiments with numerical simulations, and the modelling/observations of astrophysical jets. –> BUT IT TAKES TIME!